14 Hebbian Learning of Pulse Timing in the *Barn Owl* Auditory System

Wulfram Gerstner, Richard Kempter, J. Leo van Hemmen, and Hermann Wagner

Hebbian learning refers to an unsupervised correlation-based adaptation mechanism and is usually formulated in terms of mean firing rates. In this Chapter we study learning at the spike level. The learning process is driven by the temporal correlations between presynaptic spike arrival and postsynaptic firing.

To explore the effect of learning on pulse coding, we consider the example of auditory processing. The auditory system of the barn owl operates with a temporal precision in the microsecond range. After delay tuning, obtained by applying the learning rule to an integrate-and fire model of an auditory neuron, the temporal precision of spike firing is in the range of 20-30 microseconds. This level of precision, typical for the early stages in auditory processing, is necessary for sound source localization.

14.1 Introduction

The relevance of precise temporal spike timing in the cortex – or neural systems in general – is a fundamental, yet unsolved question [Abeles, 1994; Bialek et al., 1991; Hopfield, 1995; O'Keefe and Recce, 1993; Mainen and Sejnowski, 1995; Shadlen and Newsome, 1994; Softky, 1995; Rieke et al., 1996]; see also Chapters 1 and 4 of this book. There are, however, a few specialized subsystems for which the relevance of temporal information has been clearly shown. Prominent examples are the electro-sensory system of electric fish and the auditory system of barn owls [Carr and Konishi, 1990; Carr, 1993; Heiligenberg, 1991; Konishi, 1986; Konishi, 1993]. Here we use the latter as an example to study the following question: How can the timing of spikes be learned during early development? Specifically, how can processes of pulse generation and signal transmission be fine-tuned so as to achieve the required temporal precision?

The problem of spike-based learning arises whenever a neural system uses a strategy of temporal coding by action potentials. The auditory system is only one of several potential examples. Since we think that learning is a fundamental concept, we start in Section 2 with the problem of Hebbian learning and formulate a learning rule which operates on the level of single spikes. In Section 3 we give a quick overview of spike timing in the localization pathway of the *barn owl* auditory system. One of the key processes in the auditory system is phase locking discussed in Section 4. Finally, in Section 5, we bring the two strands, viz. Hebbian learning and auditory processing, together and apply the learning rule of Section 2 to the problem of delay tuning in the auditory system of the *barn owl*.

14.2 Hebbian Learning

14.2.1 Review of Standard Formulations

D. Hebb formulated in 1949 a fundamental principle of learning [Hebb, 1949] :

When an axon of cell A is near enough to excite a cell B and repeatedly or persistently takes part in firing it, some growth process or metabolic change takes place in one or both cells such that A's efficiency, as one of the cells firing B, is increased.

Hebb's description states that correlations between the firings of the pre- and postsynaptic neurons drive changes in the transmission efficiency. Even though the idea of learning through correlations dates further back in the past, correlation-based learning rules are now generally called Hebbian learning.

In standard neural network theory, the Hebb rule is condensed to a formula for the change of synaptic efficacy as a function of pre- and postsynaptic firing rates; see, e.g., [Hertz et al., 1991; Haykin, 1994]. Let us write ν_j for the presynaptic firing rate and ν_i for the rate of the postsynaptic neuron. Then the change Δw_{ij} of the efficacy of a connection from j to i after a learning experiment of duration $\mathcal{T}$ is

$$\Delta w_{ij} = c_{ij}\, \nu_i \nu_j + c_{ii}\, \nu_i^2 + c_{jj}\, \nu_j^2 + b_i\, \nu_i + b_j \nu_j + a\,. \qquad (14.1)$$

The first term on the right-hand side of (14.1) picks up the correlations between pre- and postsynaptic activity. The next terms are useful to impose some specific requirements like a proper normalization. The diagonal terms $c_{ii}\, \nu_i^2$ and $c_{jj}\, \nu_j^2$ are usually omitted.

As an example of (14.1), let us consider the learning rule

$$\Delta w_{ij} = \eta\, (\nu_i - \overline{\nu})\, \nu_j \qquad (14.2)$$

which is a special case of (14.1) with parameters $c_{ij} = \eta, b_i = 0, b_j = -\eta\overline{\nu}, c_{ii} = c_{jj} = a = 0$. With the rule (14.2) the direction of synaptic change (increase or decrease) reverses if the output rate ν_i crosses the reference rate $\overline{\nu}$. For $\eta < 0$, (14.2) has an interesting property. Learning tends to move the output rate ν_i towards the reference value $\overline{\nu}$. Let us consider the situation where $\nu_i < \overline{\nu}$ and $\eta < 0$. Then *all* synapses grow ($\Delta w_{ij} > 0$ for all j) with a rate proportional to ν_j. Thus the overall input strength $\propto \sum_j w_{ij}\nu_j$ increases. Stronger input raises the output rate which therefore moves in direction of $\overline{\nu}$. Inversely, if $\nu_i > \overline{\nu}$, all synaptic efficacies decrease and so does ν_i. Our spike-based learning rule, to be discussed below, will have the same property of output normalization.

The Hebb rule (14.1) may be viewed as a special case of a general learning rule [Sejnowski and Tesauro, 1989; Kohonen, 1984]

$$\Delta w_{ij} = F(w_{ij}; \nu_i, \nu_j) \qquad (14.3)$$

where F is some arbitrary function of three variables. This rule (14.3) is a *local* learning rule, since the information about pre- and postsynaptic firing rates and the present state w_{ij} of the synaptic efficacy could easily be available at the location of the synapse. (The firing rate of other neurons $k \neq i, j$, however, would be not). Expansion of (14.3) to second order in the rates ν_i, ν_j yields (14.1). As mentioned before, the diagonal terms $c_{ii}\nu_i^2$ and $c_{jj}\nu_j^2$ are often set to zero; see, e.g., [Hopfield, 1982; Linsker, 1986; Miller et al., 1989]. Hebbian learning can also be generalized to time-dependent problems, e.g., sequence learning [Sompolinsky and Kanter, 1986; Herz et al., 1988, 1989; Minai and Levy, 1993; Abbott and Blum, 1996; Blum and Abbott 1996; Wu et al., 1996; Wimbauer et al., 1994].

The expansion coefficients $a, b_i, b_j, c_{ij}, c_{ii}, c_{jj}$ may, in general, depend on w_{ij}. The functional dependence of the parameters upon w_{ij} is useful to impose weight normalization; see, for example, [Oja, 1982; Kohonen, 1984; Miller and MacKay, 1994] . To see why normalization is necessary, let us return to (14.1). The Hebb rule (14.1) gives the change of the synaptic efficacy after a single learning session of duration $\mathcal{T}$. If the experiment is repeated over a large number of trials, the weights w_{ij} can, in principle, grow without bounds. To avoid unlimited growth, we can either (i) use the w_{ij}-dependence of the coefficients to impose some weight normalization, or (ii) impose explicit upper and lower bounds for w_{ij} or (iii) renormalize the weights by hand after each trial. In the spike based learning rule discussed in the following section we have chosen the second possibility: a weight w_{ij} is not modified, if $w_{ij} + \Delta w_{ij} > w^{\max}$ or $w_{ij} + \Delta w_{ij} < 0$.

Hebbian learning is considered one of the main driving forces for neuronal organization during development. The first model studies of cortical organization development [Willshaw and von der Malsburg, 1976; Swindale 1982], have incited a long line of research, e.g., [Kohonen, 1984; Linsker, 1986abc; Miller et al., 1989; MacKay and Miller, 1990; Obermayer et al., 1992]. Most of these models use in some way or another a correlation-based unsupervised learning rule similar to (14.1) or (14.3); for a review see [Erwin et al., 1995]. Note, however, that (14.1) and (14.3) are based on a rate coding hypothesis. The exact spike timing plays no role in the learning rule. Since we want to explore pulse coding in this book, we need learning rules which take spike timing into account. Spike-based learning is the topic of the following subsection.

14.2.2 Spike-Based Learning

Hebbian learning is often vaguely described as an adaptation rule where a synapse is strengthened if pre- and postsynaptic neuron are 'simultaneously' active. In the context of pulse coding, the meaning of 'simultaneously' must be specified.

We consider a synapse from neuron j to neuron i with efficacy w_{ij}. Let us denote the presynaptic spike train by $S_j(t) = \sum_{t_j^{(f)} \in \mathcal{F}_j} \delta(t - t_j^{(f)})$ where $t_j^{(f)}$ denotes the *arrival* time at the synapse. The symbol $\mathcal{F}_j$ stands for the set of all spike arrival time at synapse j. The spike train at the output is

$S_i(t) = \sum_{t_i^{(f)} \in \mathcal{F}_i} \delta(t - t_i^{(f)})$ where $t_i^{(f)}$ are the firing times and $\mathcal{F}_i$ the set of all output spikes. A synaptic change occurs if presynaptic spike arrival and postsynaptic firing coincide within some time window; for recent experimental measurements, see [Markram et al., 1997].

A simple rectangular time window of duration $2\overline{s}$ could, for example, be described by the condition $|t_j^{(f)} - t_i^{(f)}| < \overline{s}$. More generally, we may assume in our model a learning window $W(s)$ with some arbitrary dependence upon the time difference $s = t_j^{(f)} - t_i^{(f)}$. The change of the synaptic efficacy after a learning experiment of duration $\mathcal{T}$ is then

$$\begin{aligned} \Delta w_{ij} &= \int_0^{\mathcal{T}} \int_0^{\mathcal{T}} W(t' - t)\, S_i(t)\, S_j(t')\, dt\, dt' + \\ &\quad + \tilde{b}_i \int_0^{\mathcal{T}} S_i(t)\, dt + \tilde{b}_j \int_0^{\mathcal{T}} S_j(t)\, dt + \mathcal{T}\, \tilde{a}\,. \end{aligned} \tag{14.4}$$

The first term of the right-hand side contains the learning window $W(s)$ and imposes the simultaneity constraint between presynaptic and postsynaptic firing. An example of a learning window is shown in Figure 14.1. For an interpretation of the linear terms in (14.4), we may note that $\int_0^{\mathcal{T}} S_k(t) dt = n_k$ (for $k = i, j$) is just the number of pre- or postsynaptic spikes that occur in the time window of length $\mathcal{T}$. In analogy to equation (14.1), we could add to (14.4) some diagonal terms $\tilde{c}_{ii}(t' - t) S_i(t) S_i(t') + \tilde{c}_{jj}(t' - t) S_j(t) S_j(t')$ but we will not do so.

Equation (14.4) gives the change Δw_{ij} after a learning run of duration $\mathcal{T}$. It is convenient to divide (14.4) by $\mathcal{T}$ in order to get the average rate of change

$$\begin{aligned} \frac{\Delta w_{ij}}{\mathcal{T}} &= \frac{1}{\mathcal{T}} \int_0^{\mathcal{T}} \int_{-t}^{\mathcal{T}-t} W(s)\, S_i(t)\, S_j(t+s)\, ds\, dt \\ &\quad + \frac{\tilde{b}_i}{\mathcal{T}} \int_0^{\mathcal{T}} S_i(t)\, dt + \frac{\tilde{b}_j}{\mathcal{T}} \int_0^{\mathcal{T}} S_j(t)\, dt + \tilde{a}\,. \end{aligned} \tag{14.5}$$

On the right-hand side of (14.5) we have used the substitution $s = t' - t$.

Let us suppose that the learning window $W(s)$ has some finite width $\overline{s}$. If $\mathcal{T} \gg \overline{s}$, we can extend the limits of the s-integration to $\pm\infty$ without introducing a large error. This little trick allows us to rewrite (14.5) in a nice form

$$\begin{aligned} \langle \frac{d}{dt} w_{ij} \rangle &= \int_{-\infty}^{\infty} W(s)\, \langle S_i(t)\, S_j(t+s) \rangle\, ds \\ &\quad + \tilde{b}_i\, \langle S_i(t) \rangle + \tilde{b}_j\, \langle S_j(t) \rangle + \tilde{a} \end{aligned} \tag{14.6}$$

where $\langle\, .\, \rangle$ means a temporal average over a time $\mathcal{T}$. On the left-hand side of (14.6) we have used $\langle dw_{ij}/dt \rangle = \mathcal{T}^{-1} \int_0^{\mathcal{T}} (dw_{ij}/dt) dt = \Delta w_{ij}/\mathcal{T}$. Equation (14.6) shows explicitly that the learning process is driven by the correlations $\langle S_i(t)\, S_j(t+s) \rangle$ between pre- and postsynaptic firing.

Equation (14.6) is the natural generalization of (14.1) to spike coding. To see the relation more clearly, let us assume rate coding (in the sense of a temporal average; see Chapter 1). For example, we may consider a situation where input and output spikes are generated stochastically with, respectively, rates ν_j and ν_i. Rate coding implies that (i) the rate is constant (or varies only slowly) over the learning session of duration $\mathcal{T}$ and (ii) that there are no correlations between input and output pulses apart from the correlations between the rates. Due to (i) we may use the spike count to estimate the rate, viz., $\langle S_i(t)\rangle = \nu_i$ and $\langle S_j(t)\rangle = \nu_j$. Because of (ii) we can set $\langle S_i(t)\, S_j(t+s)\rangle = \nu_i\, \nu_j$, independent of s. Thus (14.6) reduces to

$$\frac{\Delta w_{ij}}{\mathcal{T}} = \left[\int_{\infty}^{\infty} W(s)\, ds\right] \nu_i \nu_j + \tilde{b}_i \nu_i + \tilde{b}_j \nu_j + \tilde{a}\,. \tag{14.7}$$

Comparison with (14.1) yields $\int_{-\infty}^{\infty} W(s)ds = c_{ij}/\mathcal{T}$, $\tilde{b}_i = b_i/\mathcal{T}$, $\tilde{b}_j = b_j/\mathcal{T}$, $\tilde{a} = a/\mathcal{T}$, and $c_{ii} = c_{jj} = 0$.

Asymmetric learning windows have previously been used in *rate* models for hippocampal navigation [Abbott and Blum, 1996; Blum and Abbott, 1996]. Related considerations have also appeared in rate models of sequence learning [Herz et al., 1988, 1989; Minai and Levy, 1993; Wu et al., 1996]. The learning rule (14.4), however, works on the level of correlation between *pulses* in the ms range. A spike-based learning rule with short time window has also been applied to the learning of spatio-temporal pulse patterns [Gerstner et al., 1993].

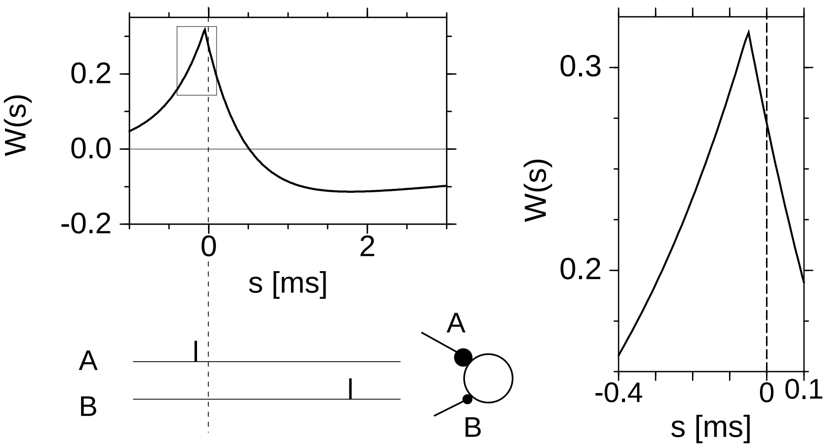

Figure 14.1. Learning Window W as a function of the delay s between postsynaptic firing and presynaptic spike arrival. The graph on the right-hand side shows the boxed region around the maximum on an expanded scale. If $W(s)$ is positive (negative) for some s, the synaptic efficacy is increased (decreased). The postsynaptic firing occurs at $s = 0$ (vertical dashed line). Learning is most efficient if presynaptic spikes arrive shortly before the postsynaptic neuron starts firing, as in synapse A. Another synapse B, which fires *after* the postsynaptic spike, is decreased. Taken from [Gerstner et al., 1996].

14.2.3 Example

In Section 5 we will use a special instance of the learning rule (14.4). We set [Gerstner et al., 1996]

$$\Delta w_{ij} = \int_0^{\mathcal{T}} \int_0^{\mathcal{T}} W(t'-t)\, S_i(t)\, S_j(t')\, dt\, dt' + \tilde{b}_j \int_0^{\mathcal{T}} S_j(t)\, dt \tag{14.8}$$

with $\tilde{b}_j > 0$ and a learning window

$$W(s) = \begin{cases} [A_+ - A_-]\, \exp[-(s^* - s)/\tau^{\mathrm{syn}}] & \text{for} \quad s < s^* \\ A_+\, \exp[-(s - s^*)/\tau_+] - A_-\, \exp[-(s - s^*)/\tau_-] & \text{for} \quad s > s^* \end{cases} \tag{14.9}$$

where $s = t_j^{(f)} - t_i^{(f)}$ is the delay between presynaptic spike arrival and postsynaptic firing. The parameters are $A_+ = 0.5, A_- = 0.2, \tau^{\mathrm{syn}} = 0.5\,\mathrm{ms}$, $\tau_+ = 0.5\,\mathrm{ms}$, $\tau_- = 5\,\mathrm{ms}$, and $s^* = -0.05\,\mathrm{ms}$. The linear term is $\tilde{b}_j = 0.1$. The learning window is plotted in Figure 14.1 and describes the following effects. If a presynaptic spike arrives slightly *before* the postsynaptic firing, the synaptic efficacy is increased ($W(s) > 0$ for $s < 0$). If a presynaptic spike arrives a few ms *after* the output spike, the synapse is weakened ($W(s) < 0$). Qualitatively, the form of the learning window (14.9) seems to be in accordance with experimental results on cortical neurons [Markram et al., 1997]. Time constants in the cortex are, however, much longer than those chosen in Figure 14.1 which is intended for neurons in the auditory pathway. In the cortex or the hippocampus, the learning window probably has a width of 50–200 ms [Bliss and Collingridge, 1993; Debanne et al., 1994].

Note that the maximum of the learning window $W(s)$ occurs for a value $s = s^* < 0$. Thus the synaptic increase is maximal if the input spike precedes the output spike by an amount $|s^*|$; see Figure 14.1. Stable learning requires that s^* be negative and of the order of the rise time of an excitatory postsynaptic potential [Gerstner et al., 1996; Kempter, 1997]. In accordance with Hebb's statement cited at the beginning of the Section, the stability requirement ensures that those synapses which are already strong and contribute most to triggering a spike receive the maximum reinforcement. The output spike occurs slightly delayed with respect to presynaptic spike arrival, and hence $s^* < 0$ must hold.

So far we have discussed the correlation term on the right-hand side of (14.8). Due to the linear term $\tilde{b}_j > 0$ each presynaptic spike has a weak positive influence on the synaptic efficacy, even if there is no output spike.

Let us now return to the rate interpretation (14.7). With the parameter settings given above we have $\int_{-\infty}^{\infty} W(s) ds < 0$ and $\tilde{b}_j > 0$. The other terms on the right-hand side of (14.7) vanish. Thus, the rate equivalent of the spike-based learning rule (14.8) is of the form (14.2) with a factor $\eta = \int W(s)\, ds < 0$. It follows from the discussion after (14.2) that the output rate will be automatically adjusted during learning to a mean level $\overline{\nu} = -\tilde{b}_j / \int W(s)\, ds$. Thus the total input $\sum_j w_{ij} \nu_j$ to neuron i remains normalized as well.

Nevertheless, individual weights could grow to very high values. To limit the growth, we have imposed upper and lower bounds, that is $\Delta w_{ij} = 0$, if $w_{ij} \geq w^{\max}$ or $w_{ij} < 0$.

14.2.4 Learning Window

In this Section we want to give a more detailed explanation for our choice of the learning window (14.9). In order to make the arguments more transparent we will consider instead of (14.9) the simple window

$$W(s) = \begin{cases} A\, \exp[-(s^* - s)/\tau^{\rm syn}] & \text{for} \quad s < s^* \\ A\, \exp[-(s - s^*)/\tau] & \text{for} \quad s > s^* \end{cases} \tag{14.10}$$

The full window (14.9) can be constructed by linear superposition of two elementary windows of the form (14.10).

On a microscopic basis, Hebbian learning is thought to involve (at least) two components. We do not wish to speculate on the chemical nature of the components, but simply call them a and b. We assume that the first component is generated by a chemical reaction chain triggered by the arrival of a spike at the synapse. As a result of the processing chain the concentration $[a]$ of component a is, after a delay Δ, increased. In the absence of further input, the concentration decays with a time constant τ_a back to its resting level $[a] = 0$. A simple way to describe this process is

$$\frac{d}{dt}[a] = -\frac{[a]}{\tau_a} + \sum_{t_j^{(f)} \in \mathcal{F}_j} \delta(t - t_j^{(f)} - \Delta)\,. \tag{14.11}$$

A high level of $[a]$ sets the synapse in a state 'ready to learn'. To generate the synaptic change and perform learning, another substance b is needed as well. The production of b is generated by a second process triggered by a *postsynaptic* spike

$$\frac{d}{dt}[b] = -\frac{[b]}{\tau_b} + \sum_{t_i^{(f)} \in \mathcal{F}_i} \delta(t - t_i^{(f)}) \tag{14.12}$$

where τ_b is another time constant. In analogy to (14.11), we could allow for a delay Δ_b in the dynamics of (14.12), but we will not do so.

Hebbian learning needs both substances to be present at the same time, thus

$$\frac{d}{dt} w_{ij}^{\rm corr} = \gamma\, [a(t)]\, [b(t)] \tag{14.13}$$

with some learning rate γ. The upper index *corr* is intended to remind the reader that we are concerned with the Hebbian correlation term only and neglect for the moment the linear terms that appear on the right-hand side of (14.4).

Let us now consider the synaptic change caused by a single presynaptic spike at $t_j^{(f)}$ and a postsynaptic spike a $t_i^{(f)} = t_j^{(f)} - s$. Integration of (14.11) and (14.12) yields

$$\begin{aligned}[a] &= \exp[-(t-t_j^{(f)}-\Delta)/\tau_a]\,\mathcal{H}(t-t_j^{(f)}-\Delta) \\ [b] &= \exp[-(t-t_i^{(f)})/\tau_b]\,\mathcal{H}(t-t_i^{(f)}) \end{aligned} \tag{14.14}$$

where $\mathcal{H}(.)$ denotes as usual the Heaviside step function. The change caused by the pair of pulses $(t_i^{(f)}, t_j^{(f)})$ and measured after a time $\mathcal{T}$ is

$$\begin{aligned}\Delta w_{ij}^{\text{corr}}(t_i^{(f)}, t_j^{(f)}) &= \int_0^{\mathcal{T}} \left(\frac{d}{dt} w_{ij}^{\text{corr}}\right) dt \\ &= \gamma \int_{t_0}^{\mathcal{T}} \exp\left[-\frac{t-t_j^{(f)}-\Delta}{\tau_a} - \frac{t-t_j^{(f)}+s}{\tau_b}\right] dt \end{aligned} \tag{14.15}$$

where $t_0 = \max\{t_j^{(f)}+\Delta, t_j^{(f)}-s\}$ and $s = t_j^{(f)} - t_i^{(f)}$. The integral in (14.15) can be performed. We introduce $s^* = -\Delta$ and find for $\mathcal{T} \gg \tau_a, \tau_b, \Delta$

$$\Delta w_{ij}^{\text{corr}}(t_i^{(f)}, t_j^{(f)}) = \begin{cases} A\,\exp[-(s^*-s)/\tau_a] & \text{for} \quad s < s^* \\ A\,\exp[-(s-s^*)/\tau_b] & \text{for} \quad s > s^* \end{cases} \tag{14.16}$$

with $A = \gamma\,(\tau_a\tau_b/\tau_a + \tau_b)$. Equation (14.16) shows that the change of the synaptic efficacy $\Delta w_{ij}^{\text{corr}}$ caused by a pair of pulses $(t_i^{(f)}, t_j^{(f)})$ depends only on the time difference $s = t_j^{(f)} - t_i^{(f)}$. We write

$$\Delta w_{ij}^{\text{corr}}(t_i^{(f)}, t_j^{(f)}) = W(t_j^{(f)} - t_i^{(f)})\,. \tag{14.17}$$

Equation (14.17) gives the change caused by a single pair of spikes. Given a train of presynaptic input spikes and a set of postsynaptic output spikes, many combinations of firing times $(t_i^{(f)}, t_j^{(f)})$ exist. Due to the linearity of the learning equation (14.13), the total change is

$$\Delta w_{ij}^{\text{corr}} = \sum_{t_i^{(f)} \in \mathcal{F}_i} \sum_{t_j^{(f)} \in \mathcal{F}_j} W(t_j^{(f)} - t_i^{(f)}) = \int_0^{\mathcal{T}} \int_0^{\mathcal{T}} W(t'-t)\, S_i(t)\, S_j(t')\, dt\, dt'\,. \tag{14.18}$$

Thus the microscopic two-component model developed in this subsection generates the correlation term on the right-hand side of the learning equation (14.4).

As mentioned before, the learning window (14.9) is slightly more complicated, since it has two phases: a positive phase of synaptic potentiation for s negative or around zero and a negative phase of synaptic depression for large s. The arguments presented in (14.11) - (14.18) would explain the positive phase only. To get both phases we must assume that the output spike triggers *two* components b_+ and b_-; the first one contributes to potentiation with intensity A_+ and the second to depression with intensity A_-. Repetition of the above steps then leads to the full learning window (14.9).

Even with this extra component, the above 'microscopic' model is still extremely simplified. In particular, it does not take into account other dynamic effects of synapses [Abbott et al., 1997; Nelson et al., 1997; Tsodyks and Markram, 1997; Markram and Tsodyks, 1996]. A fairly detailed model of these effects can be found in [Senn et al., 1997]; see also Chapter 12 in this book.

14.3 Barn Owl Auditory System

Owls hunt at night. From behavioral experiments it is known that owls can locate sound sources even in complete darkness with a remarkable precision. To do so, the signal processing in the auditory pathway must achieve a temporal precision in the microsecond range with elements that are noisy, unreliable and rather slow. In this Section we discuss the general problem of sound source localization and give a rough sketch of the auditory pathway. Sections 4 and 5 will focus on two specific aspects, viz., phase locking and delay tuning by Hebbian learning.

14.3.1 The Localization Task

Barn owls use interaural time differences (ITD) for sound source localization [Jeffress, 1948; Moiseff and Konishi, 1981; Carr and Konishi, 1990]. Behavioral experiments show that barn owls can locate a sound source in the horizontal plane with a precision of about 1-2 degrees of angle [Knudsen et al., 1979]. A simple calculation shows that this corresponds to a temporal difference of a few microseconds ($< 5\,\mu$s) between the sound waves at the left and right ear. Those small temporal differences must be detected and evaluated by the owl's auditory system; see Figure 14.2.

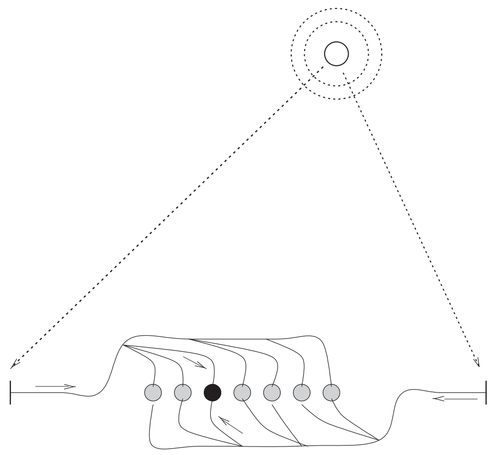

Figure 14.2. Jeffress Model. Sound waves from a source located to the right of the owl's head arrive at the two ears where they excite neuronal activity. Neuronal signals travel along transmission lines to an array of coincidence detectors. The coincidence-detecting neurons respond, if signals from both sides arrive simultaneously. Due to transmission delays, the position of the coincidence detector activiated by the signals depends on the location of the external sound source.

The basic principle of how such a time-difference detector could be set up was discussed by Jeffress about 50 years ago [Jeffress, 1948]. It consists of delay lines and an array of coincidence detectors. If the sound source is on the right-hand side of the auditory space, the sound wave arrives first at the right ear and then at the left ear. The signals propagate from both ears along transmission lines towards the set of coincidence detectors. A signal originating from a source located to the right of the owl's head, stimulates a coincidence detector on the left-hand side of the array. If the location of the signal source is shifted, a different coincidence detector responds. The 'place' of responding coincidence detectors is therefore a signature for the location of the external sound source (Figure 14.2). Such a representation has been called 'place' coding [Konishi, 1986; Carr, 1993].

Remarkably enough, such a coincidence detector circuit was found four decades later by C.E. Carr and M. Konishi [Carr and Konishi, 1990] in the nucleus laminaris of the *barn owl*. The existence of the circuit confirms the general idea of temporal difference detection by delayed coincidence measurement. It gives, however, no indication of how the precision of a few microseconds is finally achieved.

In order to better understand how precise spike timing arises, we have to look at the first few processing steps in the auditory pathway. Three aspects are important: frequency separation, phase locking, and phase-correct averaging.

14.3.2 Auditory Localization Pathway

The first few processing steps along the auditory localization pathway are sketched in Figure 14.3. The figure represents, of course, a simplified picture of auditory information processing, but it captures some essential ingredients. At both ears the sound wave is separated into its frequency components. Signals then pass an intermediate processing area called nucleus magnocellularis (NM) and meet at the nucleus laminaris (NL). Neurons there are found to be sensitive to the interaural time difference (ITD). Due to the periodicity of a sinusoidal wave, the ITD of a single frequency channel is really a *phase* difference and leaves some ambiguities. In the next processing steps further up in the auditory pathway, information on phase differences from different frequency channels is combined to retrieve the temporal difference and hence the location of the sound source in the horizontal plane. Nice reviews of the basic principles of auditory processing in the owl can be found in [Konishi, 1986, 1993; Carr, 1993] .

Let us now follow the first few processing steps in more detail. After cochlear filtering, different frequencies are processed by different neurons and stay separated up to the nucleus laminaris. In the following we may therefore focus on a single frequency channel and consider a neuron which responds best to a frequency of, say, 5 kHz.

If the ear is stimulated with a 5 kHz tone, neurons in the 5 kHz channel are activated and fire action potentials. At first sight, the spike train looks noisy. A closer look, however, reveals that the pulses are phase locked

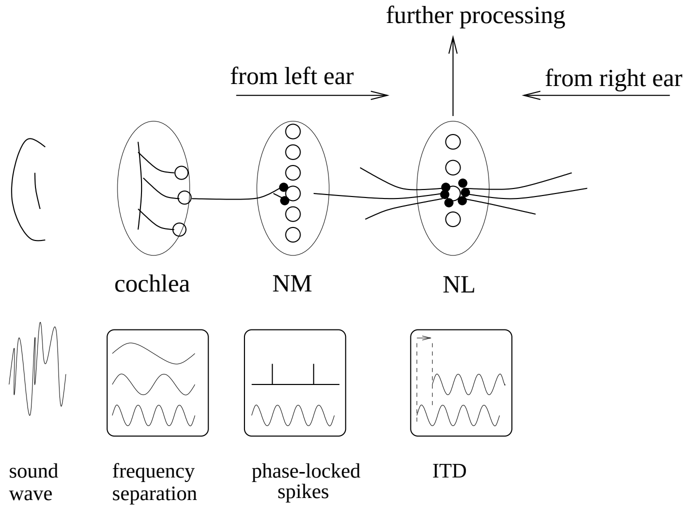

Figure 14.3. Auditory Pathway (schematic). At the cochlea a sound wave is separated into its frequency components. Phase locked spikes are transmitted along the auditory nerve to the nucleus magnocellularis (NM), an intermediate processing step. Action potentials at the output of the NM are phase locked as well. The signals from both ears meet in the nucleus laminaris (NL). Neurons in the NL are sensitive to the interaural time difference (ITD). In further processing steps, the output of neurons with different frequencies is combined to resolve remaining ambiguities.

to the stimulating tone: Spikes occur preferentially around some phase φ_0 with respect to the periodic stimulus. Phase locking is, of course, not perfect, but subject to two types of noise (Figure 14.4). First, spikes do not occur at every cycle of the 5 kHz tone. Often the neuron misses several cycles before it fires again. Second, spikes occur with a temporal jitter of about $\sigma = 40\,\mu$s around the preferred phase [Sullivan and Konishi, 1984] [Sullivan and Konishi, 1984].

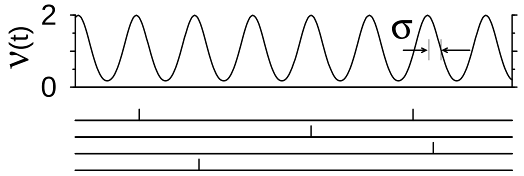

Figure 14.4. Spike trains in the auditory pathway show phase locking and can be described by a time dependent firing rate $\nu(t)$ which is modulated by the signal. Four samples of spike trains are shown at the bottom of the Figure.

To a fair approximation, we can describe the spike train by a Poisson process with a periodically modulated rate

$$\nu_j(t) = p \sum_{m=-\infty}^{\infty} \mathcal{G}_\sigma(t - m\,T - \Delta_j) \tag{14.19}$$

where T is the period of the tone (e.g., $T = 0.2\,\text{ms}$ for our 5 kHz signal), $\mathcal{G}_\sigma$ is a Gaussian with variance σ, and $\Delta_j = \varphi_j\,(T/2\pi)$ is a delay associated with the preferred phase φ_j of spikes of a given presynaptic neuron j. The amplitude p with $0 < p < 1$ is the probability of firing in one period. The temporally averaged mean firing rate is $\langle \nu_j \rangle = p/T$. The rate formula (14.19) does not take into account refractoriness of the spike trains; two spikes can be generated in arbitrary short intervals. For $p \ll 1$ short intervals are, however, unlikely and (14.19) is a useful approximation of real spike trains. In the simulations discussed in Section 5 we have imposed absolute refractoriness by requiring a minimum interspike interval of 0.5 ms. Examples of spike trains generated from (14.19) are shown in Figure 14.4.

Phase locking is seen along the auditory nerve connecting the cochlea and the nucleus magnocellularis, at the output of the nucleus magnocellularis, and also at the output of the nucleus laminaris. The phase jitter σ even decreases from one processing step to the next so that the temporal precision of phase locking increases from around $40\,\mu$s at the output of the nucleus magnocellularis to about $25\,\mu$s at the output of the nucleus laminaris. The precision of phase locking is the topic of the following subsection.

14.4 Phase Locking

14.4.1 Neuron Model

We focus on a single neuron i in the nucleus laminaris (NL). The neuron receives input from neurons in the nucleus magnocellularis (NM) through about 150 synapses. All input lines belong to the same frequency channel. The probability of spike arrival at one of the synapses is given by (14.19) where j labels the synapses and $T = 0.2\,\text{ms}$ is the period of the signal.

As a neuron model for i we take an integrate-and-fire unit (see Chapter 1.2.3) with time constant τ_m and input resistance R,

$$\tau_m \frac{du}{dt} = -u + R\,\mathcal{I}(t) \tag{14.20}$$

where the input current $\mathcal{I}(t)$ is generated by the synaptic spike input

$$\mathcal{I}(t) = \sum_j \frac{w_{ij}}{(R/\tau_m)} \sum_{t_j^{(f)} \in \mathcal{F}_j} \frac{1}{\tau_s} \exp\left(-\frac{t - t_j^{(f)}}{\tau_s} \right) \mathcal{H}(t - t_j^{(f)}) \tag{14.21}$$

where $t_j^{(f)}$ is the time of spike *arrival* at synapse j, w_{ij} is the synaptic efficacy of a connection from j to i, τ_s is a synaptic time constant, τ_m is the membrane time constant of neuron i, and $\mathcal{H}(.)$ is the Heaviside step function.

From (14.20) and (14.21) we may calculate the form of an excitatory postsynaptic potential (EPSP). The response of the membrane potential to a spike input at $s = 0$ is

$$\epsilon(s) = \frac{1}{1 - (\tau_s/\tau_m)} \left[\exp\left(-\frac{s}{\tau_m}\right) - \exp\left(-\frac{s}{\tau_s}\right) \right] \mathcal{H}(s)\,. \tag{14.22}$$

If there is repeated spike input, then the resulting EPSPs (14.22) are added until the membrane potential reaches the threshold ϑ. The moment of threshold crossing defines the firing time $t_i^{(f)}$ of an output spike. After firing, the membrane potential is reset and the summation process starts again (see Chapter 1.2.3).

From experiments on chickens it is known that the duration of an EPSP in the NL is remarkably short (< 1 ms) [Reyes et al., 1994, 1996]. Neurons of an auditory specialist like the barn owl may be even faster. In our model equations, we have set $\tau_m = \tau_s = 0.1$ ms. These values correspond to an EPSP with a duration of about 0.25 ms.

The short duration of EPSPs in neurons in the NL and NM is due to an outward rectifying current which sets in when the membrane potential exceeds the resting potential [Manis and Marx, 1991; Oertel, 1983]. The purely *passive* membrane time constant is in the range of 2 ms [Reyes et al., 1994], but the outward rectifying current reduces the effective membrane resistance whenever the voltage is above the resting potential. In a conductance-based neuron model (see Chapter 1.2.4.), all membrane currents would be described explicitly. In our integrate-and-fire model, the main effect of the outward rectifying current is taken into account by working with a short *effective* membrane time constant $\tau_m = 0.1$ ms.

A membrane constant of 0.1 ms is much shorter than that found in cortical neurons where $\tau_m \approx 10 - 50$ ms seem to be typical values; see, e.g., [Bernander et al., 1991]. Note, however, that for temporal coding in the barn owl auditory system, $\tau_m = 0.1$ ms is quite long compared to the precision of phase locking of 25 μs found in auditory neurons and necessary for successful sound source localization. How the precision of phase locking arises is the topic of the next two paragraphs.

14.4.2 Phase Locking – Schematic

To get an intuitive understanding of how phase locking arises, let us study an idealized situation and take perfectly coherent spikes as input to our model neuron (Figure 14.5).

Specifically, let us consider a situation where 100 input lines converge on the model neuron. On each line, spike arrival is given by (14.19) with $\sigma \to 0$ and $p = 0.2$. The delays Δ_j are the same for all transmission lines ($\Delta_j = \Delta_0$). Then in each cycle a volley of 20 ± 5 synchronized spikes arrive. The EPSPs evoked by those spikes are added as shown schematically in Figure 14.5. The output spike occurs when the membrane potential crosses the threshold ϑ. Note that the threshold must be reached from below. It follows that the output spike must always occur during the *rise* time of the EPSPs generated by the last bunch of spikes before firing.

Since the input spikes are phase-locked to the stimulus, the output spike will also be phase-locked to the acoustic waveform. The preferred phase of the output spike φ_i will, of course be slightly delayed with respect to the input phase $\varphi_0 = \Delta_0(2\pi/T)$. The typical delay will be less than the rise

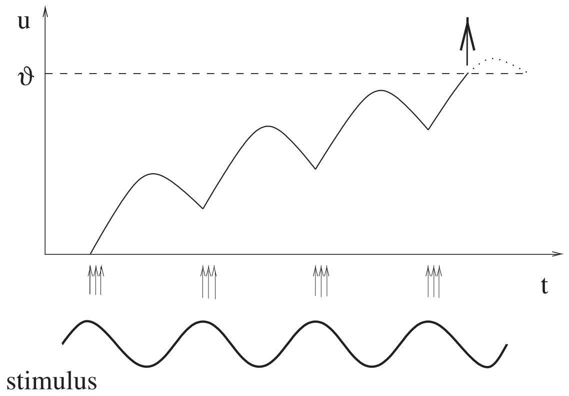

Figure 14.5. Phase Locking (schematic). Action potentials arrive periodically and are phase-locked to the stimulus in bundles of spikes (bottom). The postsynaptic potentials evoked by presynaptic spike arrival are summed and yield the total postsynaptic potential $u(t)$ which shows a pronounced oscillatory structure. Firing occurs when $u(t)$ crosses the threshold. The output spike is phase locked to the external signal, since the threshold crossing is bound to occur during a *rising* phase of u.

time $\tau_{\rm rise}$ of an EPSP. Thus, $\varphi_i = (\Delta_0 + 0.5\,\tau_{\rm rise})\,(2\pi/T)$ will be a reasonable estimate of the preferred output phase.

14.4.3 Simulation Results

Can we transfer the above qualitative arguments to a more realistic scenario? We have simulated a neuron with 154 input lines. At each synapse spikes arrive with rate (14.19). The temporal jitter has been set to $\sigma = 40\,\mu$s. The delays Δ_j (and hence the preferred phases) have a jitter of 35 μs around some mean value Δ_0. As before, $p = 0.2$ for all inputs.

A short interval taken from a longer simulation run with these input parameters is shown in Figure 14.6. Part a shows the membrane potential $u(t)$ as a function of time; Figures 14.6b and c show the distribution of spike arrival times. Even though spike arrival is rather noisy, the trajectory of the membrane potential exhibits characteristic periodic modulations. From the qualitative arguments of the preceding paragraphs, we therefore expect the output spike to be phase-locked. Figure 14.7a confirms our expectations: the distribution of output phases exhibits a pronounced peak. The width of the distribution corresponds to a temporal precision of $\sigma_{\rm out} = 25\,\mu$s, a significant increase in precision compared to the input jitter $\sigma = 40\,\mu$s.

So far we have assumed that the delays Δ_j have a small variation of 35 μs only. Hence the preferred phases $\varphi_j = \Delta_j\,(2\pi/T)$ are nearly identical for all input lines. If the preferred phases are drawn stochastically from a uniform distribution over $[0, 2\pi]$, then spike arrival at the neuron is effectively *incoherent*, even though the spikes on each input line exhibit phase-locking. If input spikes arrive incoherently, the temporal precision is lost and the output spikes have a flat phase distribution; see Figure14.7b.

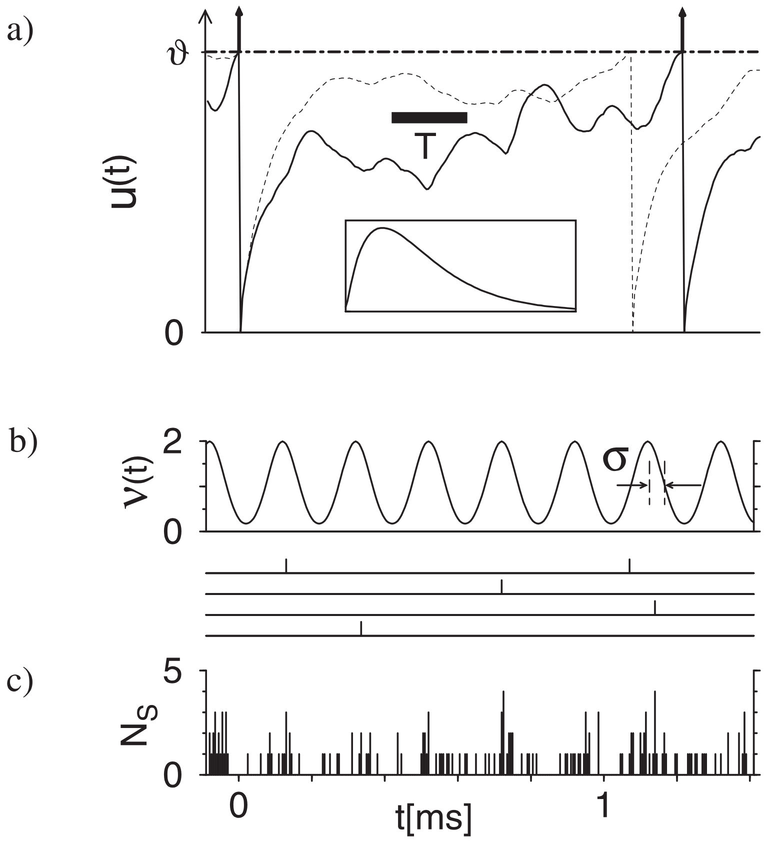

Figure 14.6. a) Membrane potential $u(t)$ of an integrate-and-fire neuron as a function of time. b) Rate $\nu_j(t)$ of presynaptic firing during 5 kHz stimulation and four samples of input spike trains (vertical bars). The model neuron receives input from 154 presynaptic neurons in volleys of phase-locked spikes with a jitter of $\sigma = 40\,\mu$s driven by a 5 kHz tone. Input spikes are generated by a stochastic process with periodically modulated rate (solid line in b)). A histogram of spike arrival times (number of spikes N_s in bins of $5\,\mu$s) summed over all 154 synapses is shown in c). Each input spike evokes an excitatory postsynaptic potential (EPSP) shown on an enlarged voltage scale (same time scale) in the inset of a). Each input spike evokes an excitatory postsynaptic potential (EPSP) shown on an enlarged voltage scale (same time scale) in the inset of a). The EPSPs from all neurons are added linearly and yield the membrane voltage u (a), main figure). With the spike input shown in c) the membrane voltage exhibits oscillations (solid line). The model neuron fires (arrow) if u reaches a threshold ϑ. Firing must always occur during the time when u increases so that, in the case of coherent input, output spikes are phase-locked as well (see also Figure 14.7a)). If input spikes arrive incoherently, $u(t)$ follows a trajectory with stochastic fluctuations but no systematic oscillations (dashed line in a)); see Figure 14.7b). Voltage in a): arbitrary units; the threshold ϑ is 36 times the amplitude of a single EPSP. Rate in b) in kHz. Taken from [Gerstner et al., 1996].

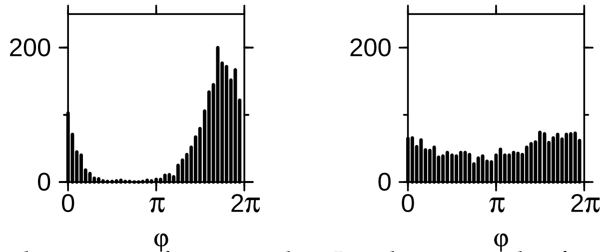

Figure 14.7. Phase histograms of output spikes. In a the input spikes from the 154 presynaptic neurons arrive *coherently* with the spiking statistics as shown in Figs. 6*b* and 6*c*. In this case, the distribution of output spikes exhibits a pronounced maximum indicating a high degree of phase locking. The width of the peak corresponds to a temporal precision of $25\,\mu$s. b If input spikes arrive incoherently, the histogram of output phases has no significant structure. Taken from [Gerstner et al., 1996].

We conclude that integrate-and-fire neurons are capable of transmitting phase information. Output spikes are generated with high temporal precision, if input spikes arrive with a high degree of coherence. If input spikes arrive incoherently, the temporal information is lost. The consequences of these observations are discussed in the following Section.

14.5 Delay Tuning by Hebbian Learning

14.5.1 Motivation

Each neuron in the nucleus laminaris (NL) of the barn owl receives input from about 150 presynaptic neurons [Carr and Konishi, 1990; Carr, 1993]. The high degree of convergence enables the neuron to increase the signal-to-noise ratio by averaging over many (noisy) transmission lines. As we have seen in the preceding Section, the temporal precision of phase locking is indeed increased from $40\,\mu$s in the input lines to $25\,\mu$s in the output of our model neuron in the NL.

Such an averaging scheme, however, can work only, if the preferred phases φ_j of all input lines are (nearly) the same. Otherwise the temporal precision is decreased or even lost completely as shown in Figure 14.7*b*. To improve the signal-to-noise ratio, 'phase-correct' averaging is needed. The question arises of how a neuron in the NL can perform correct averaging.

The total delay from the ear to the NL has been estimated to be in the range of 2–3 ms [Carr and Konishi, 1990]. Even if the transmission delays vary by only 0.1–0.2 ms between one transmission line and the next, the phase information of a 5 kHz signal is completely lost when the signals arrive at the NL. Therefore the delays must be precisely tuned so as to allow the neurons to perform phase-correct averaging. Tuning of delays may be achieved by an unsupervised Hebbian mechanism discussed in the following subsection.

14.5.2 Selection of Delays

Precise wiring of the auditory connections could be set up genetically. This is, however, rather unlikely since the owl's head grows considerably during development. Moreover, while neurons in the nucleus laminaris of the adult owl are sensitive to the interaural phase difference, no such sensitivity was found for young owls [Carr, 1995; see also Chuhma and Ohmori, 1998]. This indicates that delay tuning arises only later during development. It is clear that there can be no external supervisor or controller that selects the appropriate delays. What the owl needs is an adaptive mechanism which can be implemented locally and which achieves a tuning of appropriate delays.

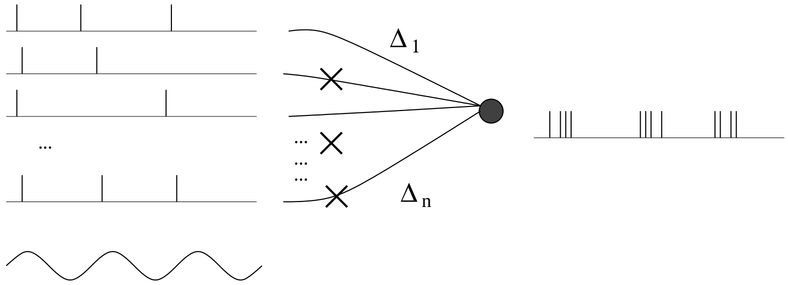

Figure 14.8. Unsupervised Learning mechanism (schematic). Several transmission lines converge on a single coincidence detector neuron in the nucleus laminaris. When pulses are generated at the ear, they are phase locked to the external sound wave (left part of figure). In order to achieve a high temporal resolution, pulses should *arrive* synchronously at the coincidence detector neuron which is possible only if the delays of the transmission lines are finely tuned. An unsupervised adaptive mechanism selects and reinforces some of the transmission lines and suppresses other (black crosses). After learning, pulses arrive with a high degree of coherence (right).

The basic idea of the learning model is sketched in Figure 14.8. Immediately after birth a large number of connections are formed. During an early period of post-natal development a tuning process takes place which selectively reinforces transmission lines with similar preferred phase and eliminates others.

To achieve this selection process, we have used the spike based Hebbian learning rule discussed in Section 2. The time window $W(s)$ is given by (14.9) and shown in Figure 14.1. The maximum of $W(s)$ is located at $s^* = -0.05\,\text{ms}$. The choice $s^* = -\tau_{\text{rise}}/2$ guarantees stable learning [Gerstner et al., 1996; Kempter, 1997].

The results of a simulation run are shown in Figure 14.9. Before learning the neuron receives input over about 600 synapses from presynaptic neurons. Half of the input lines originate from the left, the other half from the right ear. The total transmission delays Δ_j are different between one line and the next and vary between 2 and 3 ms. At the beginning of learning all synaptic efficacies have the same strength $w_{ij} = 1$.

Both ears are stimulated by a pure 5 kHz tone with interaural time difference ITD = 0. The effect of stimulation is that spikes arrive at the synapses with periodically modulated rate $\nu_j(t)$ given by (14.19). During learning, synaptic weights are modified according to the Hebbian learning rule (14.8). The homogeneous distribution ($w_{ij} = 1$ for all j) becomes unstable during learning (Figure 14.9, Middle). The instability has also been confirmed analytically [Kempter, 1997].

After learning the synaptic efficacies have approached either the upper bound $w_{\max} = 3$ or they have decayed to zero. The transmission lines which remain after learning have either very similar delays, or delays differing by a full period (Figure 14.9, Bottom).

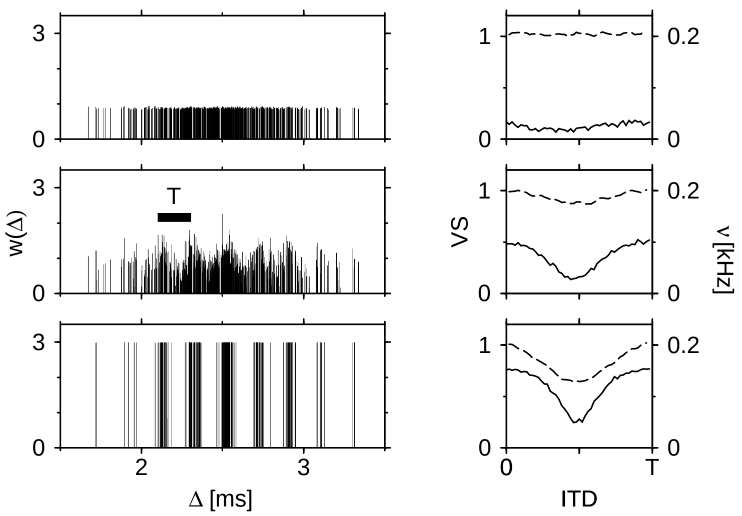

Figure 14.9. Development of tuning to a 5kHz tone. The left column shows the strength of synaptic efficacies w_{ij} of all synapses. Synapses are indexed according to the delay Δ_j of the corresponding transmission line and are plotted as $w_{ij} = w(\Delta)$. On the right, we show the vector strength (vs, solid line) and the output firing rate (ν, dashed) as a function of the interaural time delay (ITD). **Top**. Before learning, there are 600 synapses (300 from each ear) with different delays, chosen randomly from a Gaussian distribution with mean 2.5 ms and variance 0.3 ms. All weights have unit value. The output is not phase-locked ($vs \approx 0.1$) and shows no dependence upon the ITD.**Middle**. During learning, some synapses are strengthened others decreased. Those synapses which increase have delays that are similar or that differ by multiples of the period $T = 0.2$ ms of the stimulating tone. The vector strength of the output increases and starts to depend on the ITD. **Bottom**. After learning, only about 150 synapses ($\approx$ 75 from each ear) survive. Both the output firing rate ν and the vector strength vs show the characteristic dependence upon the ITD as seen in experiments with adult owls [Carr and Konishi, 1990]. The neuron has the maximal response ($\nu = 200$ Hz) for ITD = 0, the stimulus used during the learning session of the model neuron. The vector strength at ITD = 0 is $vs \approx 0.8$ which corresponds to a temporal precision of 25 μs. Taken from [Gerstner et al. 1997.]

The sensitivity of the output firing rate to the interaural time difference (ITD) and the degree of phase locking were tested before, during, and after learning (right column in Figure 14.9). Before learning, the neuron shows no sensitivity to the ITD. This means that the neuron is not a useful coincidence detector for the sound source localization task. During learning ITD sensitivity develops similar to that found in experiments [Carr, 1995]. After learning the output rate is significantly modulated as a function of ITD. The response is maximal for ITD = 0, the ITD used during learning. The form of the ITD tuning curves corresponds to experimental measurements.

To test the degree of phase locking in the output we have plotted the vector strength, vs, as a function of ITD. By definition the vector strength is proportional to the first Fourier component of the histogram of phase distributions; cf. Figure 14.7. It is therefore a suitable measure of phase-locking. The vector strength vs is normalized so that $vs = 1$ indicates perfect phase locking (infinite temporal precision or $\sigma_{\mathrm{out}} = 0$).

Let us focus on the value of vs in the case of optimal stimulation (ITD = 0). Before learning $vs \approx 0.1$, which indicates that there is no significant phase locking. The value of $vs \approx 0.8$ found after learning confirms that after the tuning of the synapses, phase locking is very pronounced.

14.6 Conclusions

In this Chapter we have studied the auditory system of the barn owl as an example of neural pulse coding. In our simplified model, we have seen that the generation of action potentials is very precise, if input spikes *arrive* coherently at the synapses. Coherent input causes large systematic fluctuations of the total input current to the neuron. A temporally modulated input current has also been successfully used in an experimental preparation to generate precisely timed spike output [Mainen and Sejnowski, 1995].

In a general setting, the condition of coherent spike arrival may seem rather artificial. We have seen, however, that a Hebbian learning rule may automatically select and reinforce those synapses which support coherent spike arrival and suppress others.

In the peripheral stages of the auditory system, neurons are extremely fast with an effective membrane time constant in the range of 0.1 ms. In cortex or hippocampus neurons are slower with time constants in the range of 10–50 ms [Bernander et al., 1991]. To translate the results of this Chapter to other areas, we would therefore have to multiply all time scales by a factor of 100. A temporal precision of 20–30 μs for auditory neurons then implies a precision of 2–3 ms for spike timing in other areas. This is still a remarkably fast time scale and would support the idea of synfire chain activity [Abeles, 1991, 1994; Lestienne, 1996].

The spike-based learning rule used in this Chapter is an example of a Hebbian learning rule. Temporal aspects of Hebbian learning have been previously studied in models of sequence learning and completion in associative memory models, for path planning in hippocampal models, and for the development of spatio-temporal receptive fields [Sompolinsky and

Kanter, 1986; Herz et al., 1988, 1989; Abbott and Blum, 1996; Blum and Abbott 1996; Wu et al., 1996; Wimbauer et al., 1994]. The formulation of this Chapter is different since it is based on pulse timing and not on time-dependent firing rates. A related spike-based learning rule has been used for learning of spatio-temporal pulse patterns [Gerstner et al., 1993].

Qualitatively, the form of the Hebbian learning window used in the simulations seems to be in agreement with experimental results [Bliss and Collingridge, 1993; Debanne et al., 1994; Markram et al., 1997] even though the time scale is different. Spike-based Hebbian learning may be seen as a special case of the general problem of synaptic dynamics [Abbott et al., 1997; Nelson et al., 1997; Tsodyks and Markram 1997; Markram and Tsodyks, 1997; Senn et al., 1997]. The next few years will certainly bring a better insight into this fascinating topic.

References

[Abbott and Blum, 1996] Abbott, L. F. and Blum, K. I. (1996). Functional significance of long-term potentiation for sequence learning and prediction. *Cerebral Cortex*, 6:406–416.

[Abbott et al., 1997] Abbott, L. F., Varela, J. A., Sen, K., and Nelson, S. B. (1997). Synaptic depression and cortical gain control. *Science*, 275:220–224.

[Abeles, 1991] Abeles, M. (1991). *Corticonics*. Cambridge University Press, Cambridge.

[Abeles, 1994] Abeles, M. (1994). Firing Rates and Well-Timed Events. In *Models of Neural Networks 2*, E. Domany, K. Schulten, and J. L. van Hemmen, eds., Springer, New York, chapter 3, 121–140.

[Bialek et al., 1991] Bialek, W., Rieke, F., de Ruyter van Stevenick, R. R., and Warland, D. (1991). Reading a neural code. *Science*, 252:1854–1857.

[Bliss and Collingridge, 1993] Bliss, T. V. P. and Collingridge, G. L. (1993). A synaptic model of memory: Long-term potentiation in the hippocampus. *Nature*, 361:31–39.

[Blum and Abbott, 1996] Blum, K. I. and Abbott, L. F. (1996). A model of spatial map formation in the hippocampus of the rat. *Neural Computation*, 8:85–93.

[Carr, 1995] Carr, C. E. (1995). The development of nucleus laminaris in the barn owl. *Advances in Hearing Research*, Manley, G. A., Klump, G. M., Köppl, C., Fastl, H., and Oeckinghaus, H., eds., World Scientific, Singapore, 24–30.

[Carr and Konishi, 1990] Carr, C. E. and Konishi, M. (1990). A circuit for detection of interaural time differences in the brain stem of the barn owl. *J. Neurosci.*, 10:3227–3246.

[Carr, 1993] Carr, C. E. (1993). Processing of temporal information in the brain. *Ann. Rev. Neurosci.*, 16:223–243.

[Chuma and Ohmori, 1998] Chuhma, N. and Ohmori, H. (1998). Postnatal development of phase-locked high-fidelity synaptic transmission in the medial nucleus of the trapezoid body of the rat. *J. Neurosci.*, 18:512–520.

[Debanne et al., 1994] Debanne, D., Gähwiler, B. H., and Thompson, S. M. (1994). Asynchronous pre- and postsynaptic activity induces associative long-term depression in area CA1 of the rat hippocampus in vitro. *Proc. Natl. Acad. Sci. USA*, 91:1148–1152.

[Erwin et al., 1995] Erwin, E., Obermayer, K., and Schulten, K. (1995). Models of orientation and ocular dominance columns in the visual cortex: a critcal comparison. *Neural Computation*, 7:425–468.

[Gerstner and Abbott, 1997] Gerstner, W. and Abbott, L. F. (1997). Learning navigational maps through potentiation and modulation of hippocampal place cells. *J. Comput. Neurosci.*, 4:79–94.

[Gerstner et al., 1993] W. Gerstner, R. Ritz, and J. L. van Hemmen. Why spikes? Hebbian learning and retrieval of time–resolved excitation patterns. *Biol. Cybern.*, 69:503–515.

[Gerstner et al., 1996] Gerstner, W., Kempter, R., van Hemmen J. L., and Wagner, H. (1996). A neuronal learning rule for sub-millisecond temporal coding. *Nature*, 383:76–78.

[Gerstner et al., 1997] Gerstner, W., Kempter, R., van Hemmen J. L., and Wagner, H. (1997). A developmental learning rule for coincidence tuning in the barn owl auditory system. *Computational Neuroscience: trends in research 1997*, J. Bower, ed., Plenum Presss, New York, 665–669.

[Haykin, 1994] Haykin, S. (1994). *Neural Networks*. Prentice Hall, Upper Saddle River, NJ.

[Hebb, 1949] Hebb, D. O. (1949). *The Organization of Behavior*. Wiley, New York.

[Heiligenberg, 1991] Heiligenberg, W. (1991). *Neural Nets in Electric Fish*. MIT Press, Cambridge.

[Hertz et al., 1991] Hertz, J., Krogh, A., and Palmer, R. G. (1991). *Introduction to the Theory of Neural Computation*. Addison-Wesley, Redwood City CA.

[Herz et al., 1988] Herz, A. V. M., Sulzer, B., Kühn, R., and van Hemmen, J. L. (1988). The Hebb rule: Representation of static and dynamic objects in neural nets. *Europhys. Lett.*, 7:663–669.

[Herz et al., 1989] Herz, A. V. M., Sulzer, B., Kühn, R., and van Hemmen, J. L. (1989). Hebbian learning reconsidered: Representation of static and dynamic objects in associative neural nets. *Biol. Cybern.*, 60:457–467.

[Hopfield, 1982] Hopfield, J. J. (1982). Neural networks and physical systems with emergent collective computational abilities. *Proc. Natl. Acad. Sci. USA*, 79:2554–2558.

[Hopfield and Herz, 1995] Hopfield, J. J. and Herz, A. V. M. (1995). Rapid local synchronization of action potentials: towards computation with coupled integrate-and-fire networks. *Proc. Natl. Acad. Sci. USA*, 92:6655.

[Jeffress, 1948] Jeffress, L. A. (1948). A place theory of sound localisation. *J. Comp. Physiol. Psychol.*, 41:35–39.

[O'Keefe amd Recce, 1993] O'Keefe, J. and Recce, M. (1993). Phase relationship between hippocampal place units and the hippocampal theta rhythm. *Hippocampus*, 3:317–330.

[Kempter, 1997] Kempter, R. (1997). *Hebbsches Lernen zeitlicher Codierung: Theorie der Schallortung im Hörsystem der Schleiereule*. Naturwissenschaftliche Reihe, Bd. 17. DDD, Darmstadt.

[Knudsen et al., 1979] Knudsen, E. I., Blasdel, G. G., and Konishi, M. (1979). Sound localization by the barn owl (tyto alba) measured with the search coil technique. *J. Comp. Physiol.*, 133:1–11.

[Kohonen, 1984] Kohonen, T. (1984). *Self-Organization and Associative Memory*. Springer-Verlag, New York.

[Konishi, 1986] Konishi, M. (1986). Centrally synthesized maps of sensory space. *Trends Neurosci.*, 9:163–168.

[Konishi, 1993] Konishi, M. (1993). Listening with two ears. *Scientific American*, 34–41.

[Lestienne, 1996] Lestienne, R. (1996). Determination of the precision of spike timing in the visual cortex of anaesthetised cats. *Biol. Cybern.*, 74:55–61.

[Linsker, 1986a] Linsker, R. (1986). From basic network principles to neural architecture: emergence of spatial-opponent cells. *Proc. Natl. Acad. Sci. USA*, 83:7508–7512.

[Linsker, 1986b] Linsker, R. (1986). From basic network principles to neural architecture: emergence of orientation selective cells. *Proc. Natl. Acad. Sci. USA*, 83:8390–8394.

[Linsker, 1986c] Linsker, R. (1986). From basic network principles to neural architecture: emergence of orientation columns. *Proc. Natl. Acad. Sci. USA*, 83:8779–8783.

[MacKay and Miller, 1990] MacKay, D. J. C. and Miller, K. D. (1990). Analysis of Linsker's application of Hebbian rules to linear networks. *Network*, 1:257–297.

[Mainen and Sejnowski, 1995] Mainen, Z. F. and Sejnowski, T. J. (1995). Reliability of spike timing in neocortical neurons. *Science*, 268:1503–1506.

[Manis and Marx, 1991] Manis, P. B. and S. O. Marx, (1991). Outward currents in isolated ventral cochlear nucleus neurons. *J. Neurosci.*, 11:2865–2880.

[Markram and Tsodyks, 1996] Markram, H. and Tsodyks, M. (1996). Redistribution of synaptic efficacy between neocortical pyramidal neurons. *Nature*, 382:807–810.

[Markram et al., 1997a] Markram, H., Lübke, J., Frotscher, M., and Sakmann, B. (1997). Regulation of synaptic efficacy by coincidence of postsynaptic APs and EPSPs. *Science*, 275:213–215.

[Markram and Tsodyks, 1997b] Markram, H. and Tsodyks, M. (1997). The information content of action potential trains: a synaptic basis. *Artificial Neural Networks - ICANN'97*, Springer, Lecture Notes in Computer Science, 1327.

[Miller and MacKay, 1994] Miller, K. D. and MacKay, D. J. C. (1994). The role of constraints in Hebbian learning. *Neural Computation*, 6:100–126.

[Miller et al., 1989] Miller, K. D., Keller, J. B., and Stryker, M. P. (1989). Ocular dominance column development: analysis and simulation. *Science*, 245:605–615.

[Minai and Levy, 1993] Minai, A. A. and Levy, W. B. (1993). Sequence learning in a single trial. *Proc. World Congress on Neural Networks II*, 505–508.

[Moiseff and Konishi, 1981] Moiseff, A. and Konishi, M. (1981). Neuronal and behavioral sensitivity to binaural time differences in the owl. *J. Neurosci.*, 1:40–48.

[Nelson et al., 1997] Nelson, S. B., Varela, J. A., Sen, K., and Abbott, A. F. (1997). Functional significance of synaptic depression between cortical neurons. In J. Bower, editor, *Computational Neuroscience - Trends in Research 1997*, Plenum Press, 429–434.

[Oertel, 1983] Oertel, D. (1983). Synaptic responses and electrical properties of cells in brain slices of the mouse anteroventral cochlear nucleus. *J. Neurosci.*, 3:2043–2053.

[Oja, 1982] Oja, E. (1982). A simplified neuron model as a principal component analyzer. *J. Math. Biol.*, 15:267–273.

[Reyes et al., 1994] Reyes, A. D., Rubel, E. W., and Spain, W. J. (1994). Membrane properties underlying the firing of neurons in the avian cochlear nucleus. *J. Neurosci.*, 14:5352–5364.

[Reyes et al., 1996] Reyes, A. D., Rubel, E. W., and Spain, W. J. (1996). In vitro analysis of optimal stimuli for phase-locking and time-delayed modulation of firing in avian nucleus laminaris neurons. *J. Neurosci.*, 16:993–1007.

[Rieke et al., 1996] Rieke, F., Warland, D., de Ruyter van Steveninck, R. R., and Bialek, W. (1996). *Spikes – Exploring the Neural Code*. MIT Press, Cambridge, MA.

[Sejnowski, 1989] Sejnowski, T. J. and Tesauro, G. (1989). The Hebb rule for synaptic plasticity: algorithms and implementations. In J. H. Byrne and W. O. Berry, eds., *Neural Models of Plasticity*, Academic Press, chapter 6, 94–103.

[Senn et al., 1997] Senn, W., Tsodyks, M., and Markram, H. (1997). An algorithm for synaptic modification based on exact timing of pre-and postsynaptic action potentials. *Artificial Neural Networks - ICANN'97*, Springer, Lecture Notes in Computer Science 1327:121–126.

[Shadlen and Newsome, 1994] Shadlen, M. N. and Newsome, W. T. (1994). Noise, neural codes and cortical organization. *Curr. Opin. Neurobiol.*, 4:569–579.

[Softky, 1995] Softky, W. R. (1995). Simple codes versus efficient codes. *Curr. Opin. Neurobiol.*, 5:239–247.

[Sompolinsky and Kanter, 1996] Sompolinsky, H. and Kanter, I. (1996). Temporal association in asymmetric neural networks. *Phys. Rev. Lett.*, 57:2861–2864.

[Sullivan and Konishi, 1984] Sullivan, W. E. and Konishi, M. (1984). Segregation of stimulus phase and intensity coding in the cochlear nucleus of the barn owl. *J. Neurosci.*, 4:1787–1799.

[Swindale, 1982] Swindale, N. V. (1982). A model for the formation of orientation columns. *Proc. R. Soc. Lond. B*, 215:211–230.

[Tsodyks and Markram, 1997] Tsodyks, M. and Markram, H. (1997). Neurotransmitter release probability determines the nature of the neural code between neocortical pyramidal neurons. *Proc. Natl. Acad. Sci., USA*, 94:719–723.

[Willshaw and von der Malsburg, 1976] Willshaw, D. J. and von der Malsburg, C. (1976). How patterned neuronal connections can be set up by self-organization. *Proc. R. Soc. Lond. B*, 194:431–445.

[Wimbauer et al., 1994] Wimbauer, S., Gerstner, W., and van Hemmen, J. L. (1994). Emergence of spatio-temporal receptive fields and its application to motion detection. *Biol. Cybern.*, 72:81–92.

[Wu et al., 1996] Wu, X., Baxter, R. A., and Levy, W. B. (1996). Context codes and the effect of noisy learning on a simplified hippocampal CA3 model. *Biol. Cybern.*, 74:159–165.